


## Article

# Effect of Variation in Viscosity on Static and Dynamic Characteristics of Rough Porous Journal Bearings with Micropolar Fluid Squeeze Film Lubrication

Neminath Bhujappa Naduvinamani <sup>1,\*</sup>  and Bhagyashri Kotreppa Koppa <sup>2</sup><sup>1</sup> Department of Mathematics, Gulbarga University, Kalaburagi 585106, India<sup>2</sup> Government Pre-University College, Cholachagudda, Bagalakote 587201, India; bhagyakoppa820@gmail.com

\* Correspondence: naduvinamaninb@yahoo.co.in

**Abstract:** In the present study, an effort was made to determine the effects of a porous matrix with different viscosities on the dynamic and static behaviors of rough short journal bearings taking into account the action of a squeezing film under varying loads without journal rotation. The micropolar fluid was regarded as a lubricant that contained microstructure additives in both the porous region and the film region. By applying Darcy's law for micropolar fluids through a porous matrix and stochastic theory related to uneven surfaces, a standardized Reynolds-type equation was extrapolated. Two scenarios with a stable and an alternating applied load were analyzed. The impacts of variations in viscosity, the porous medium, and roughness on a short journal bearing were examined. We inspected the dynamic and static behaviors of the journal bearing. We found that the velocity of the journal center with a micropolar fluid decreased when there was a cyclic load, and the impact of variations in the viscosity and porous matrix diminished the load capacity and pressure in the squeeze film and increased the velocity of the journal center.

**Keywords:** micropolar fluid; journal bearings; porous; surface roughness; viscosity variation; dynamic loading



**Citation:** Naduvinamani, N.B.; Koppa, B.K. Effect of Variation in Viscosity on Static and Dynamic Characteristics of Rough Porous Journal Bearings with Micropolar Fluid Squeeze Film Lubrication. *Lubricants* **2024**, *12*, 389. <https://doi.org/10.3390/lubricants12110389>

Received: 14 October 2024

Revised: 10 November 2024

Accepted: 11 November 2024

Published: 13 November 2024



**Copyright:** © 2024 by the authors. Licensee MDPI, Basel, Switzerland. This article is an open access article distributed under the terms and conditions of the Creative Commons Attribution (CC BY) license (<https://creativecommons.org/licenses/by/4.0/>).

## 1. Introduction

Rotating machines are widely used to transform rotating energy from various sources into efficient energy. One rotating segment is distinct from the machine's stationary portion in these rotating machines, which is achieved by using bearings. The bearings permit the surfaces of the rotating part to slide relative to the stationary part. The concept of a bearing was originally proposed by Lord Rayleigh [1] in 1918. One of the most prevalent kinds of hydrodynamic bearings is the journal bearing: supporting a rotating shaft is its primary purpose. These bearings are utilized in virtually every type of machinery that rotates, not only with static loads, such as the load and weight of rotors induced by transmitted torque of reduction gears, additionally close to only machine element consequently being capable to suppress numerous incredible forces functioning on a revolving shaft. With the development of large, multistage rotating machines that are now also high-speed, compact, and highly efficient, the magnitude and variability of the stimulating forces have increased with the bearing load. As a result, the role and significance of journal bearings have greatly expanded. The basic mathematics of a full journal bearing have been recognized since 1904 when Sommerfeld developed the complete solution for the infinite journal from Reynold's 1886 theory. The detailed applications of the theory of a full journal bearing was discussed by Cameron and Wood [2]. The concept of a journal bearing and its importance was discussed by Tipei [3]. Lidia et al. [4] conducted an experimental investigation into the effect of surface texture on journal bearing performance. Rotating machinery is often subject to vibrations due to critical speeds, imbalance, and instability. Usually, the least expensive modification to make to a machine is to alter the bearing. Journal bearings for

rotating machinery were designed by Allaire and Flack [5]. Sunil et al. [6] theoretically described the influence of lubricants on the performance of journal bearings.

Researchers are examining non-Newtonian fluids currently. A micropolar fluid is one that includes rigid particle suspensions, like those found in blood, liquid crystals, certain colloidal fluids, and dirty oil. Additionally, these fluids have a microstructure. Eringen [7,8] was the first to propose micropolar fluid theory. The theory of lubrication for micropolar fluids was examined by Kline and Allen [9]. Zaheeruddin and Isa [10] theoretically described a micropolar- fluid-lubricated one-dimensional journal bearing. Micropolar liquid lubrication and its effects on short journal bearings were studied by Nicolae Tipei [11]. Bujurke et al. [12] looked into micropolar-fluid-lubricated squeeze film. The effects of a micropolar lubricant on partial journal bearings were examined by Sharma et al. [13]. Boualem et al. [14] analyzed the effects of the interplay between piezo-viscous dependence and elastic deformation on the working of a journal bearing with a non-Newtonian fluid.

Later, interest in porous bearings increased extremely swiftly due to their self-lubricating behavior, lower maintenance requirement, pressure generation, enhanced damping properties, etc. Due to their self-lubricating features, for the duration of an engine's life, a porous bearing does not need additional lubrication because of their porous zones filled with lubricants. The lubrication of finite porous journal bearings was described by Murti [15]. A porous media model using a modified Reynolds equation was derived by Li [16]. Anas et al. [17] conducted a numerical simulation of a finite flexible porous journal bearing lubricated with non-Newtonian coupled stress fluid. Dhanapal et al. [18] described the effects of squeeze film lubrication on porous secant curved circular plates induced by micropolar fluids. Bhattacharjee et al. [19] theoretically analyzed a micropolar fluid-lubricated single-layered porous short journal bearing. A comparative discussion of micropolar-fluid-lubricated double- and single-layered journal bearings with different porosities was reported by Bhattacharjee et al. [20].

During the past few years, the examination of the influence of uneven surfaces on numerous bearing surfaces has been the focus of research. In the mechanical field, the impact of surface roughness has long been studied, since surface irregularities influence the formation of nucleation, leading to cracks or rust. Over the past few decades, a number of tribology researchers have studied the impacts of the roughness of bearing surfaces. Stochastic strategies have been used to mathematically model the texture of surfaces with random structures. Christensen [21] developed a stochastic method for studying the effects of the lubrication of rough surfaces on hydrodynamic bearings. Zhu et al. [22] studied the impacts of surface roughness and inappropriate non-Newtonian fluid lubrication on compliant journal bearings. The influence of surface roughness on the dynamic performance of a Rayleigh step bearing lubricated with coupled stress fluid was determined by Naduvinamani and Ashwini [23]. Finite partial rough journal bearings lubricated with micropolar fluid considering the squeezing effect and porosity were considered by Monayya and Santosh [24]. Chaitra et al. [25] examined the properties of rough, curved annular plates in the presence of micropolar lubricants under the influence of the squeezing effect for different porosities. The impact of porosity and roughness on finite journal bearing lubricated with a micropolar lubricant was observed by Ujjal et al. [26].

As a bearing works, the viscosity  $\mu$  is constant despite originating from both temperature and pressure. The viscosity of all liquids, specifically of hydrocarbon lubricants, deteriorates with increasing temperature. The changes in viscosity with variation in temperature are important in numerous practical scenarios where lubricants are required to function over a wide range of temperatures. Temperature-related changes in the viscosity of oil cannot be accurately predicted with mathematical relationships. As a result of the formulas used for defining the viscosity–temperature relationship are purely empirical; for precise computations, lubrication engineers need experimental data.

In the present study, it was assumed that thermal equilibrium exists and that the viscosity varies with temperature according to a given law. The viscosity–temperature

relationship can be described by a relationship between the viscosity and the film thickness. This assumption was made on the basis of the experimental validation by Tipei [3], as the highest temperature occurs in zones where the film is the thinnest. When the viscosity  $\mu_1^*$  at  $H = h_1$  is known, then  $\mu = \mu_1^* \left(\frac{H}{h_1}\right)^Q$ , where  $Q$  typically lies between 0 and 1 based on the nature of the lubricant. However, in this paper, various numerical values are assumed for  $Q$  in order to discuss the effects of variations in viscosity without carrying out detailed thermal calculations. Sinha et al. [27] suggested that the influence of viscosity variations can be attributed to the subsidiary fluid in journal bearings. The effect of viscosity variations on the non-Newtonian lubrication of a squeeze film conical bearing with a porous wall, studied with a Rabinowitsch fluid model, was analyzed by Rao and Rahul [28]. Zheng et al. [29] determined the effects of oil film thickness and viscosity on the performance of misaligned journal bearings with coupled stress lubricants. Squeeze film lubrication analysis and the optimization of a porous annular disk with different viscosities of a non-Newtonian fluid were observed with the Rabinowitsch fluid model by Rahul et al. [30]. Vishwanath et al. [31] applied a multigrid approach to determine the combined impact of roughness and variation in viscosity on journal bearing lubrication with a squeeze film.

Several researchers have recently been investigating the dynamic and static properties on different types of bearings. Lin [32] focused on the dynamic–static characteristics of coupled stress fluid-lubricated journal bearings protected by squeeze films. Gu et al. [33] theoretically and numerically investigated the static properties of aerostatic journal bearings with changes in porosity. The impact of non-Newtonian lubricants on the dynamic and static properties of journal bearings was explained by Dang et al. [34]. Journal bearings must provide sufficient damping and be stiff enough to impede bearing-contributed vibration and to produce appropriate gear retention, which affect rotor system dynamics. Fang et al. [35] determined the line collision damping and stiffness characteristics of bearings with transient elasto-hydrodynamic lubrication. The effect of variations in viscosity on the squeeze film performance of a narrow hydrodynamic journal bearing with coupled stress fluid was reported by Jaya Chandra Reddy [36]. The viscosity of fluid lubricants was discussed by Ajimokotan [37]. Under uncertainty, the dynamic and static characteristics of journal bearings were discussed by Chao et al. [38]. Sharma and Krishna [39] described the dynamic and static manifestations of an offset bearing with a micropolar lubricant.

In the current work, we studied the impacts of viscosity variations and porosity on the static and dynamic behaviors of rough short journal bearings lubricated with micropolar fluids under squeezing action, which, to the best of our knowledge, has not yet been studied.

## 2. Formulation

Figure 1 displays a schematic diagram of the bearing under study.  $R$  is the journal radius with zero rotation that arrives at the surface of a bearing with specific velocity  $\left(\frac{\partial h}{\partial t}\right)$  at any point along the circumferential segment  $\theta$ . The roughness of the surface of a film of thickness  $H$  can be calculated as follows:

$$H = h(\theta) + h_s^* \quad (1)$$

where  $h(\theta) = c[1 + \varepsilon \cos \theta]$  is the average film thickness,  $c$  is the radial clearance,  $\varepsilon (= \frac{e}{c})$  is the eccentricity parameter ratio, and  $h_s^*$  is stochastic in nature and governed by the probability density function  $f(h_s^*)$  measured over the interval  $(-c^*, c^*)$ , where  $c^*$  is the maximum deviation from the average thickness of the film. The mean  $\alpha_1^*$ , standard deviation  $\sigma_1^*$ , and parameter  $\varepsilon_1^*$ , which is a measure of the symmetry about a random variable  $h_s^*$ , are defined by the relationships given by Andharia et al. [40,41]:

$$\alpha_1^* = E[h_s^*] \quad (2)$$

$$\alpha_1^{*2} = E[(h_s^* - \alpha_1^*)^2] \quad (3)$$

$$\varepsilon_1^* = E[(h_s^* - \alpha_1^*)^3] \tag{4}$$

where  $E$  is an expectancy operator, which is defined by

$$E(\bullet) = \int_{-\infty}^{\infty} (\bullet)f(h_s^*)dh_s^* \tag{5}$$

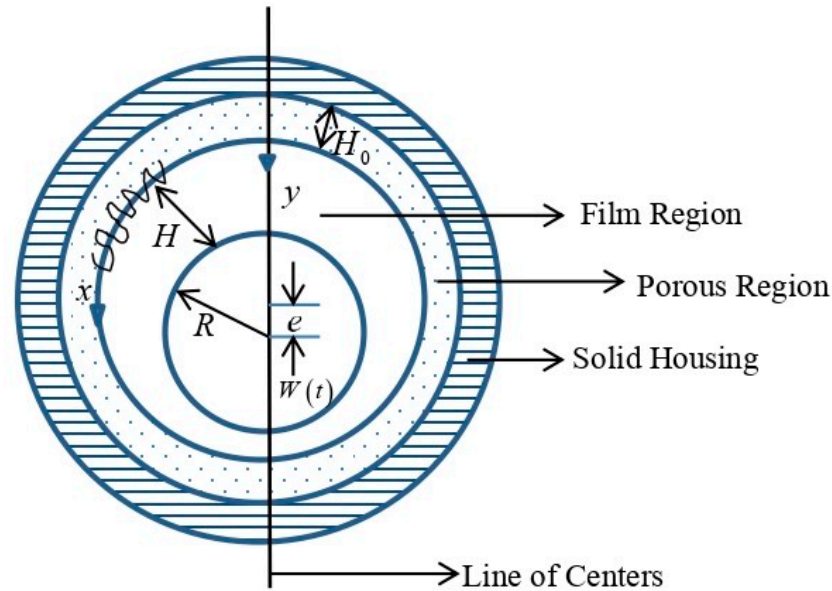


Figure 1. Geometrical configuration of the considered bearing.

The factors  $\sigma_1^*$ ,  $\alpha_1^*$ , and  $\varepsilon_1^*$  are not dependent on  $x$ . The mean  $\alpha_1^*$  and parameter  $\varepsilon_1^*$  can take both positive and negative values;  $\sigma_1^*$  can only take positive values. A symmetrical distribution is considered in the specific case of  $\varepsilon_1^* = 0$ . Positive and negative values of  $\varepsilon_1^*$  indicate bearing surfaces with positively skewed and negatively skewed roughness, respectively.

Using lubrication theory, the fundamental equations proposed by Eringen [3] for micropolar fluids are provided:

$$\left(\mu + \frac{\chi}{2}\right) \frac{\partial^2 u}{\partial y^2} + \chi \frac{\partial v_3^*}{\partial y} - \frac{\partial p}{\partial x} = 0 \tag{6}$$

$$\frac{\partial p}{\partial y} = 0 \tag{7}$$

$$\left(\mu + \frac{\chi}{2}\right) \frac{\partial^2 w}{\partial y^2} - \chi \frac{\partial v_1^*}{\partial y} - \frac{\partial p}{\partial z} = 0 \tag{8}$$

The conservation of angular momentum is calculated as

$$\gamma \frac{\partial^2 v_1^*}{\partial y^2} - 2\chi v_1^* + \chi \frac{\partial w}{\partial y} = 0 \tag{9}$$

$$\gamma \frac{\partial^2 v_1^*}{\partial y^2} - 2\chi v_1^* - \chi \frac{\partial u}{\partial y} = 0 \tag{10}$$

The formula for mass conservation is

$$\frac{\partial u}{\partial x} + \frac{\partial v}{\partial y} + \frac{\partial w}{\partial z} = 0 \tag{11}$$

where  $\mu$  is a coefficient of Newtonian viscosity;  $\chi, \gamma$  are the viscosity of the spin and the viscosity coefficient for micropolar fluids;  $u, v$ , and  $w$  are the velocity components along the  $x, y$ , and  $z$  directions, respectively; and  $v_1^*, v_2^*$ , and  $v_3^*$  are the micro-rotational velocity components.

The modified Darcy's law, which considers the impacts of polarity, governs the movement of lubricants with micropolarity through a porous medium. This type of flow is represented by

$$\vec{q}_1^* = \frac{-k_1^*}{(\mu + \chi)} \nabla p^* \quad (12)$$

where  $\vec{q}_1^* = (u^*, v^*, w^*)$  is the modified Darcy velocity vector, along with

$$u^* = \frac{-k_1^*}{(\mu + \chi)} \frac{\partial p_1^*}{\partial x}, v^* = \frac{-k_1^*}{(\mu + \chi)} \frac{\partial p_1^*}{\partial y}, w^* = \frac{-k_1^*}{(\mu + \chi)} \frac{\partial p_1^*}{\partial z} \quad (13)$$

where  $k_1^*$  is the porous matrix's permeability, and  $p_1^*$  is the porous region's pressure, which, as a result of the continuity of fluid in porous media, satisfies the Laplace equation.

$$\frac{\partial^2 p_1^*}{\partial x^2} + \frac{\partial^2 p_1^*}{\partial y^2} + \frac{\partial^2 p_1^*}{\partial z^2} = 0 \quad (14)$$

The pertinent boundary conditions are

i. at  $y = 0$  (the bearing's surface) and

$$u = 0, v = v^*, w = 0 \quad (15a)$$

$$v_1^* = 0, v_3^* = 0 \quad (15b)$$

ii. at  $y = H$  (the journal's surface)

$$u = 0, v = \frac{\partial H}{\partial t}, w = 0 \quad (16a)$$

$$v_1^* = 0, v_3^* = 0 \quad (16b)$$

The solutions to Equations (6) and (8)–(10) are subject to the related circumstances noted in Equations (15a), (15b), (16a) and (16b) as

$$u = \frac{1}{\mu} \left( \frac{y^2}{2} \frac{\partial p}{\partial x} + A_{11}y \right) - \frac{2N^2}{m} \times [A_{21} \sinh(my) + A_{31} \cosh(my)] + A_{41} \quad (17)$$

$$w = \frac{1}{\mu} \left( \frac{y^2}{2} \frac{\partial p}{\partial z} + A_{12}y \right) - \frac{2N^2}{m} \times [A_{22} \sinh(my) + A_{32} \cosh(my)] + A_{42} \quad (18)$$

$$v_1^* = \frac{1}{2\mu} \left( y \frac{\partial p}{\partial z} + A_{12} \right) + A_{22} \cosh(my) + A_{32} \sinh(my) \quad (19)$$

$$v_3^* = A_{21} \cosh(my) + A_{31} \sinh(my) - \frac{1}{2\mu} \left( y \frac{\partial p}{\partial x} + A_{11} \right) \quad (20)$$

where

$$A_{11} = 2\mu A_{21}$$

$$A_{21} = \frac{A_{31} \sinh(mH) - \left[ \frac{(H)}{(2\mu)} \right] \left[ \frac{(\partial p)}{(\partial x)} \right]}{1 - \cosh(mH)}$$

$$A_{12} = -\frac{H}{2\mu} \frac{\partial p}{\partial z} \left\{ H \sinh(mH) + \frac{2N^2}{m} [1 - \cosh(mH)] \right\} \times \frac{1}{A_5}$$

$$\begin{aligned}
 A_{12} &= -\frac{H}{2\mu} \frac{\partial p}{\partial z} \left\{ H \sinh(mH) + \frac{2N^2}{m} [1 - \cosh(mH)] \right\} \times \frac{1}{A_5} \\
 A_{22} &= \frac{A_{12}}{2\mu} \\
 A_{31} &= \frac{H}{2\mu} \frac{\partial p}{\partial x} \left\{ \frac{H}{2} [\cosh(mH) - 1] + H - \frac{N^2}{m} \sinh(mH) \right\} \times \frac{1}{A_5} \\
 A_{32} &= \frac{1}{\mu} \frac{\partial p}{\partial z} \left\{ \frac{H}{2} [\cosh(mH) - 1] + H - \frac{N^2}{m} \sinh(mH) \right\} \times \frac{1}{A_5} \\
 A_{41} &= \frac{2N^2}{m} A_{31} \\
 A_{42} &= \frac{2N^2}{m} A_{32} \\
 A_5 &= \frac{H}{\mu} \left\{ \sinh(mH) - \frac{2N^2}{mH} [\cosh(mH) - 1] \right\} \\
 \text{in which } m &= \frac{N}{l}, N = \left( \frac{\chi}{\chi + 2\mu} \right)^{\frac{1}{2}}, l = \left( \frac{\gamma}{4\mu} \right)^{\frac{1}{2}}
 \end{aligned}$$

where  $N$  is a dimensionless coupling number that describes the coupling regarding the angular and linear momentum equations. When  $N$  is equal to zero, the linear momentum equations reduce to the classical Navier–Stokes equation, where the linear and angular momentum equations decouple. Parameter  $l$  is a dimension length that can be interpreted as the lubricant molecule's dimensions. Here, when  $l \rightarrow 0$ , the microstructure disintegrates completely.

By integrating Equation (14) over the thickness  $H_0$  of the porous layer with respect to  $y$  and utilizing the pertinent boundary conditions related to a solid backing ( $\frac{\partial p_1^*}{\partial y} = 0$ ) at  $y = -H_0$ , we obtain

$$\left. \frac{\partial p_1^*}{\partial y} \right|_{y=0} = - \int_{-H_0}^0 \left( \frac{\partial^2 p_1^*}{\partial x^2} + \frac{\partial^2 p_1^*}{\partial z^2} \right) dy \quad (21)$$

Assume that the thickness of the porous layer,  $H_0$ , is an extremely small. Utilizing the pressure continuity condition ( $p = p_1^*$ ) at the interface ( $y = 0$ ) of the porous medium and lubricant film, Equation (21) reduces to

$$\left. \frac{\partial p_1^*}{\partial y} \right|_{y=0} = -H_0 \left( \frac{\partial^2 p}{\partial x^2} + \frac{\partial^2 p}{\partial z^2} \right) \quad (22)$$

At the interface ( $y = 0$ ), velocity component of specific Darcy's velocity  $v_1^*$  is then provided by

$$v_1^*|_{y=0} = \frac{k_1^* H_0}{(\mu + \chi)} \left( \frac{\partial^2 p}{\partial x^2} + \frac{\partial^2 p}{\partial z^2} \right) \quad (23)$$

Integrating the equation of continuity (11) over the thickness of the film with respect to  $y$ , we obtain a specific Reynolds-type equation. Additionally, substituting  $u$  and  $w$  into Equation (11) with their related formulations in Equations (17) and (18), as well as utilizing the boundary conditions in Equations (15a) and (16a), as obtained by Naduvanamani and Santosh [42] for the smooth case, we obtain

$$\begin{aligned}
 \frac{\partial}{\partial x} \left\{ \left[ f(N, l, H) + \frac{12\mu k_1^* H_0}{(\mu + \chi)} \right] \frac{\partial p}{\partial x} \right\} + \\
 \frac{\partial}{\partial z} \left\{ \left[ f(N, l, H) + \frac{12\mu k_1^* H_0}{(\mu + \chi)} \right] \frac{\partial p}{\partial z} \right\} = 12\mu \frac{\partial H}{\partial t} \quad (24)
 \end{aligned}$$

where

$$f(N, l, H) = H^3 + 12l^2H - 6NlH^2 \coth\left(\frac{NH}{2l}\right)$$

$$\frac{\partial H}{\partial t} = c \frac{\partial \varepsilon}{\partial t} \cos \theta$$

When Equation (24) is multiplied by  $f(h_s^*)$  on both sides, using Equations (2)–(4) and integrating from  $-c^*$  to  $c^*$  with respect to  $h_s^*$ , the averaged specific Reynolds equation can be acquired as follows:

$$\frac{\partial}{\partial x} \left\{ \left[ F(N, l, h) + \frac{12\mu k_1^* H_0}{(\mu + \chi)} \frac{\partial E(p)}{\partial x} \right] \right\} + \frac{\partial}{\partial z} \left\{ \left[ F(N, l, h) + \frac{12\mu k_1^* H_0}{(\mu + \chi)} \frac{\partial E(p)}{\partial z} \right] \right\} = 12\mu \frac{\partial h}{\partial t} \tag{25}$$

$$F(N, l, h) = E[f(N, l, H)] \approx F_1^* + F_2^*(F_3^* + F_4^*) \tag{26}$$

$$F_1^* = h^3 + \varepsilon_1^* + 3h^2\alpha_1^* + 3h(\alpha_1^{*2} + \sigma_1^{*2}) + 3\alpha_1^*\sigma_1^{*2} + \alpha_1^{*3} + 12l^2(h + \alpha_1^*)$$

$$F_2^* = -6Nl(h^2 + \alpha_1^{*2} + \sigma_1^{*2} + 2h\alpha_1^*)$$

$$F_3^* = \left\{ 1 - \text{Coth}^2\left(\frac{Nh}{2l}\right) \right\} \times \left\{ \frac{N\alpha}{2l} - \frac{N^3}{24l^3} (\varepsilon_1^* + \alpha_1^{*3} + 3\alpha_1^*\sigma_1^{*2}) \right\}$$

$$F_4^* = \text{Coth}\left(\frac{Nh}{2l}\right) \left\{ 1 - \frac{N^2}{4l^2} (\alpha_1^{*2} + \sigma_1^{*2}) \right\}$$

and

$$\frac{\partial h}{\partial t} = c \frac{\partial \varepsilon}{\partial t} \cos \theta$$

### 3. Short Journal Bearing

When comparing axial variations in pressure, circumferential variations are neglected when employing short journal bearing approximations. As a result, the averaged Reynolds-type Equation (25) reduces to

$$\frac{\partial}{\partial z} \left[ \left( F(N, l, h) + \frac{12\mu k_1^* H_0}{(\mu + \varepsilon)} \right) \frac{\partial E(p)}{\partial z} \right] = 12\mu \frac{\partial h}{\partial t} \tag{27}$$

It is now assumed that the fluid film thickness  $H$  is affected by variations in Newtonian viscosity  $\mu$ .

$$\mu = \mu_1^* \left( \frac{H}{h_1} \right)^Q \tag{28}$$

where  $\mu_1^*$  is the inlet viscosity at  $H = h_1 = c(1 + \varepsilon)$ . The exponent  $Q$  is calculated as

$$Q = \frac{\log\left(\frac{\mu_1^*}{\mu_2^*}\right)}{\log\left(\frac{h_1}{h_2}\right)} \tag{29}$$

In relation to film thickness  $h_2$ ,  $\mu_2^*$  is the outlet viscosity. The specific lubricant being used determines the parameter  $Q$  ( $0 \leq Q \leq 1$ ); for a perfect Newtonian fluid,  $Q = 0$ , while for perfect gases,  $Q = 1$ . For mathematical ease, it is assumed that the coupling number  $N$  and characteristic length parameter  $l$  are not dependent on the variation in viscosity. This can be achieved by assuming that  $\chi$  and  $\gamma$  differ in the same manner as  $\mu$ . In the present analysis, the effect of variations in viscosity is considered in the fluid film region, as the squeezing effects are predominant in the film region. The porous region is isotropic and has a constant thickness and hence the Newtonian variation in viscosity is considered to be negligible in comparison to the viscosity variations in the film region (i.e.,  $Q = 0$ ).

Substituting Equation (28) in Equation (27), we obtain

$$\frac{\partial}{\partial z} \left[ \left( F(N, l, h) + \frac{12\mu k_1^* H_0}{(\mu + \chi)} \right) \frac{\partial E(p)}{\partial z} \right] = 12\mu_1^* \left( \frac{H}{h_1} \right)^Q \frac{\partial h}{\partial t} \quad (30)$$

Using the dimensionless scheme, we have

$$\begin{aligned} \theta &= \frac{x}{R}, \bar{z} = \frac{z}{L}, \bar{l} = \frac{l}{c}, \bar{h} = \frac{h}{c}, \varepsilon_1 = \frac{\varepsilon_1^*}{c}, \alpha = \frac{\alpha_1^*}{c} \\ \sigma^2 &= \frac{\sigma_1^{*2}}{c^2}, \bar{p} = \frac{E(p)c^2}{\mu_1^* R^2 \left( \frac{d\varepsilon}{dt} \right)}, \bar{k} = \frac{k_1^*}{c^2}, \bar{H}_0 = \frac{H_0}{c}, \\ \psi &= \frac{k_1^* H_0}{c^3}, N = \left( \frac{\chi}{(\chi + 2\mu)} \right)^{\frac{1}{2}} \end{aligned}$$

A dimensionless representation of the modified averaged Reynolds Equation (30) is as follows:

$$\begin{aligned} \frac{\partial}{\partial \bar{z}} \left\{ \left[ \bar{F}(N, \bar{l}, \bar{h}) + 12\psi \left( \frac{1 - N^2}{1 + N^2} \right) \right] \frac{\partial \bar{p}}{\partial \bar{z}} \right\} &= 12 \cos \theta \frac{\bar{h}^Q}{(1 + \varepsilon)^Q} \\ \bar{F}^*(N, \bar{l}, \bar{h}) &\approx \bar{F}_1^* + \bar{F}_2^* (\bar{F}_3^* + \bar{F}_4^*) \end{aligned} \quad (31)$$

where

$$\bar{F}_1^* = \bar{h}^3 + \varepsilon_1 + 3\bar{h}^2 \alpha + 3\bar{h}(\alpha^2 + \sigma^2) + 3\alpha\sigma^2 + \alpha^3 + 12\bar{l}^2(\bar{h} + \alpha)$$

$$\bar{F}_2^* = -6N\bar{l}(\bar{h}^2 + \alpha^2 + \sigma^2 + 2\bar{h}\alpha)$$

$$\bar{F}_3^* = \left\{ 1 - \text{Coth}^2 \left( \frac{N\bar{h}}{2\bar{l}} \right) \right\} \times \left\{ \frac{N\alpha}{2\bar{l}} - \frac{N^3}{24\bar{l}^3} (\varepsilon_1 + \alpha^3 + 3\alpha\sigma^2) \right\}$$

and

$$\bar{F}_4^* = \text{Coth} \left( \frac{N\bar{h}}{2\bar{l}} \right) \left\{ 1 - \frac{N^2}{4\bar{l}^2} (\alpha^2 + \sigma^2) \right\}$$

The pressure's pertinent boundary conditions are

$$\bar{p} = 0 \text{ at } \bar{z} = \pm 0.5 \quad (32)$$

Equation (31) changes to the following form when the boundary conditions (32) are met:

$$\bar{p} = \frac{6 \cos \theta (z^2 - 0.25)}{F(N, \bar{l}, \bar{h}) + 12\psi \left( \frac{1 - N^2}{1 + N^2} \right)} \frac{\bar{h}^Q}{(1 + \varepsilon)^Q} \quad (33)$$

Here, the journal bearing has zero rotation. Integrate the mean film pressure  $E(p)$  to obtain the average load capacity  $E(W)$ , which is expressed as

$$E[W(t)] = -2R \int_{z=0}^{-L} \int_{\theta=\frac{\pi}{2}}^{\frac{3\pi}{2}} E(p) \cos \theta d\theta dz \quad (34)$$

Because a squeeze film generates an average load  $E(W(t))$  equal to the applied load  $W_s$ , when a bearing operates under steady load  $W_s$ ,

$$E[W(t)] = W_s \quad (35)$$



The journal center's locus is found as follows by entering Equations (33) and (35) into Equation (34).

$$\begin{aligned}\bar{W} &= \frac{E[W(t)]}{\mu LR \left( \frac{d\varepsilon}{dt} \right)} = \int_{\theta=\frac{\pi}{2}}^{\theta=\frac{3\pi}{2}} \frac{\cos^2 \theta (1 + \varepsilon \cos \theta)^Q}{\left[ F(N, \bar{l}, \bar{h}) + 12\psi \left[ \frac{(1-N^2)}{(1+N^2)} \right] \right]} (1 + \varepsilon)^Q d\theta \\ &= G(\varepsilon, N, \bar{l}, \alpha, \sigma, \varepsilon_1)\end{aligned}\quad (36)$$

In several practical programs, under dynamic circumstances, a squeeze film operates with a journal bearing. In these situations, the rotational center's path varies with fluctuations in the applied load. Here, the time-dependent applied load is treated as a sinusoidal function.

$$E(W(t)) = W_0 \sin(\omega t) \quad (37)$$

Here,  $W_0$  represents the amplitude and  $\omega$  represents the frequency of the oscillations in the load.

Substituting Equations (36) and (37) into Equation (35), the locus of the journal center is acquired as follows:

$$\frac{d\varepsilon}{d\tau} = \frac{30 \sin \tau}{\pi S' G(\varepsilon, N, \bar{l}, \alpha, \sigma, \varepsilon_1)} \quad (38)$$

where

$$S' = \frac{\mu N}{\left( \frac{W_0}{2LR} \right)} \left( \frac{R}{C} \right)^2, \tau = \omega t = \frac{2\pi N}{60} t$$

#### 4. Results and Discussion

The present study explored the impact of variations in porosity, viscosity, and roughness on the dynamic and static behaviors of a journal bearing lubricated with a micropolar fluid. The dimensionless factors  $\bar{l}$  and  $N$  express the impact of the micropolar lubricant. Specifically,  $N \left( = \left( \frac{\chi}{\chi + 2\mu} \right)^{\frac{1}{2}} \right)$  is the coupling number, which indicates the coupling of rotational and linear motion during the micro-rotation of the subsidiaries contained within the fluid. The dimensionless factor for the characteristic length  $\bar{l} \left( = \frac{l}{c} \right)$  describes the relationship of the fluid with the geometry of the bearing. The impact of permeability is described by the dimensionless permeability coefficient,  $\psi \left( = \frac{kH_0}{c^3} \right)$ ; moreover, as  $\psi \rightarrow 0$ , the permeability affects the related solid case. The roughness factor influences the squeeze film's properties;  $Q$  impacts the viscosity; and  $\alpha$ ,  $\varepsilon_1$  and  $\sigma$  are dimensionless parameters describing the effects of the roughness of the bearing surface. The significance of such factors depends on the squeeze film being used.

##### 4.1. Pressure Distribution

The effects of the variation in the dimensionless mean film pressure  $\bar{p}$  with the circumferential coordinate  $\theta$  and viscosity factor  $Q$  under two distinct permeability parameters  $\psi$  for  $N = 0.7$ ,  $\alpha = 0.01$ ,  $\sigma = 0.15$ ,  $\varepsilon_1 = -0.01$ , and  $\bar{l} = 0.2$  are presented in Figure 2. The required dimensionless pressure  $\bar{p}$  of the squeeze film diminishes with increasing viscosity parameter  $Q$ . The impact of the porous layer decreases the dimensionless pressure in the squeeze film with increasing permeability factor  $\psi$ . The impact of micropolarity on the changes in the dimensionless mean pressure  $\bar{p}$  of the film with  $\theta$  is shown in Figures 3 and 4. It was confirmed that  $\bar{p}$  notably increases with rising values of  $N$  and  $\bar{l}$  in the solid region compared to the porous region when  $\alpha = 0.01$ ,  $\sigma = 0.15$ ,  $\varepsilon_1 = -0.01$ ,  $\varepsilon = 0.01$ ,  $Q = 0.5$ . The influence of roughness parameters  $\alpha$  and  $\varepsilon_1$  when the viscosity parameter  $Q = 0.5$  on the

variations in  $\bar{p}$  with  $\theta$  is depicted in Figures 5 and 6. We proved that the dimensionless pressure  $\bar{p}$  is higher with a negatively skewed surface roughness in solid regions than in porous regions, where it is lower for a positively skewed surface roughness. Furthermore,  $\bar{p}$  decreases more with increasing values of  $\sigma$  in porous regions than in solid regions, as shown in Figure 7.

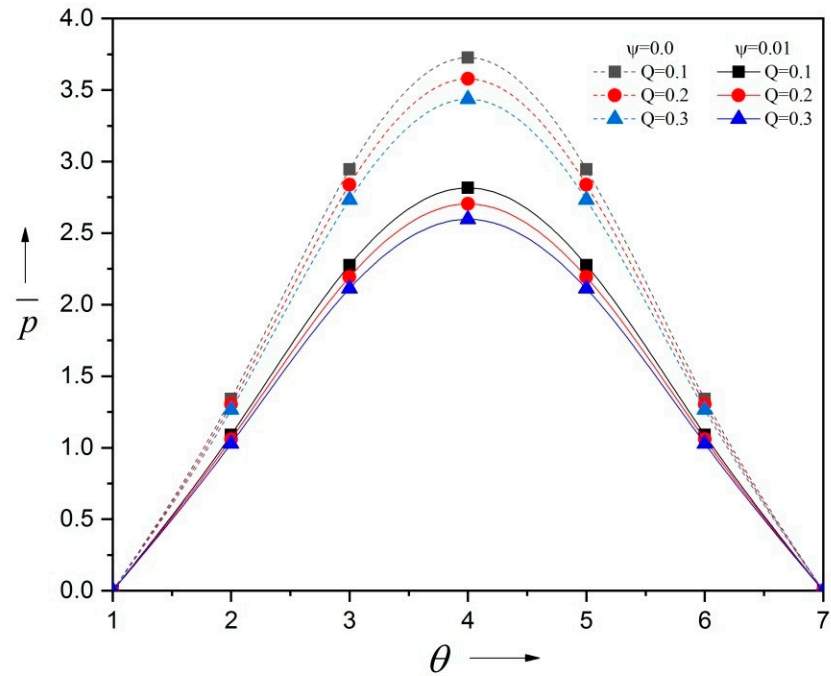


**Figure 2.** Variation in dimensionless pressure  $\bar{p}$  as a function of  $\theta$  for distinct values of viscosity parameters  $Q$  and  $\psi$ .

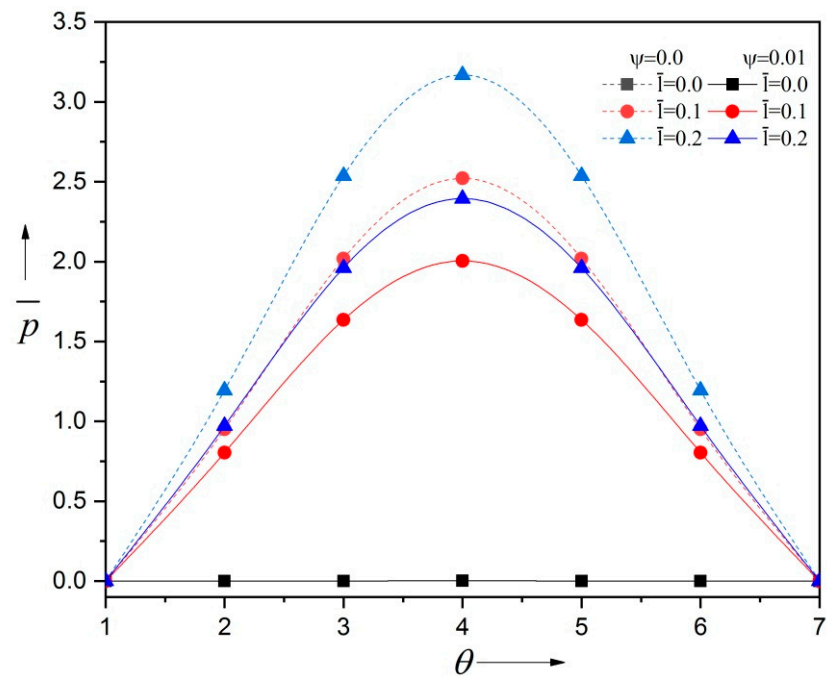


**Figure 3.** Variation in dimensionless pressure  $\bar{p}$  with respect to  $\theta$  for various values of  $\bar{l}$  and  $\psi$  when  $\epsilon_1 = -0.01, \sigma = 0.15, \alpha = 0.01, Q = 0.5$  and  $N = 0.7$ .

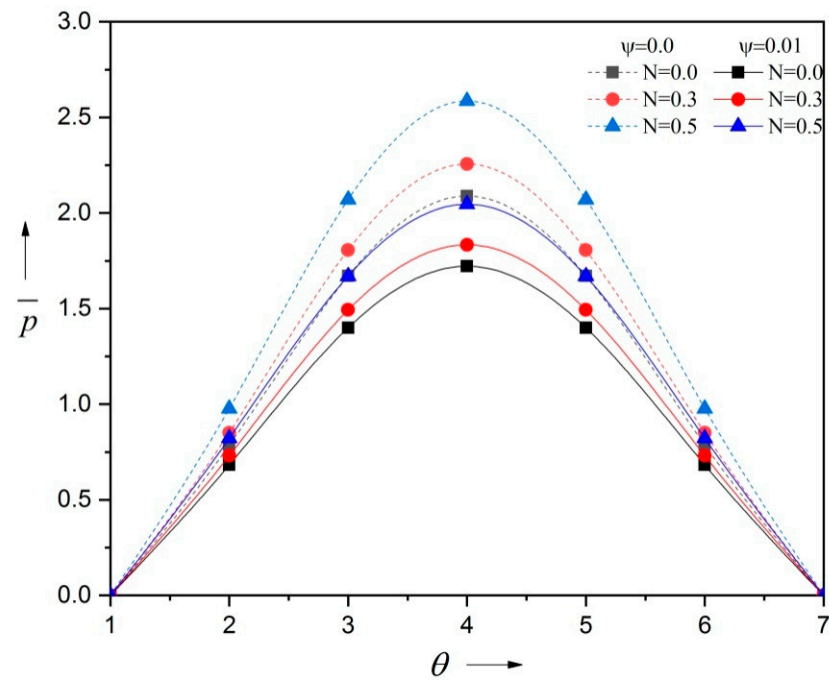


**Figure 4.** Variation in dimensionless pressure  $\bar{p}$  in relation to  $\theta$  for different values of  $N$  and  $\psi$  when  $\varepsilon_1 = -0.01, \sigma = 0.15, \alpha = 0.01, Q = 0.5$  and  $\bar{l} = 0.2$ .

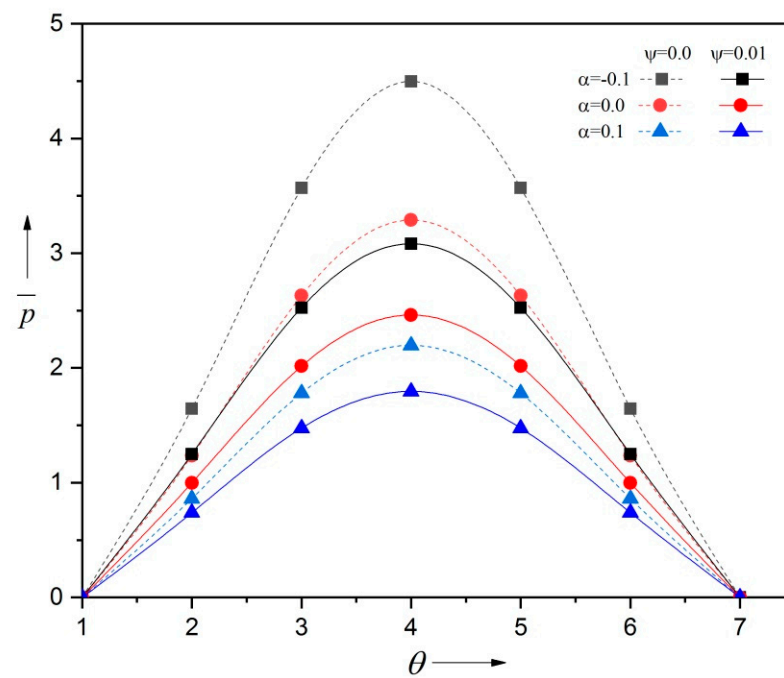


**Figure 5.** Variation in dimensionless pressure  $\bar{p}$  with  $\theta$  for distinct values of  $\alpha$  and  $\psi$  when  $\sigma = 0.15, \varepsilon_1 = -0.01, Q = 0.5, \bar{l} = 0.2$ , and  $N = 0.7$ .

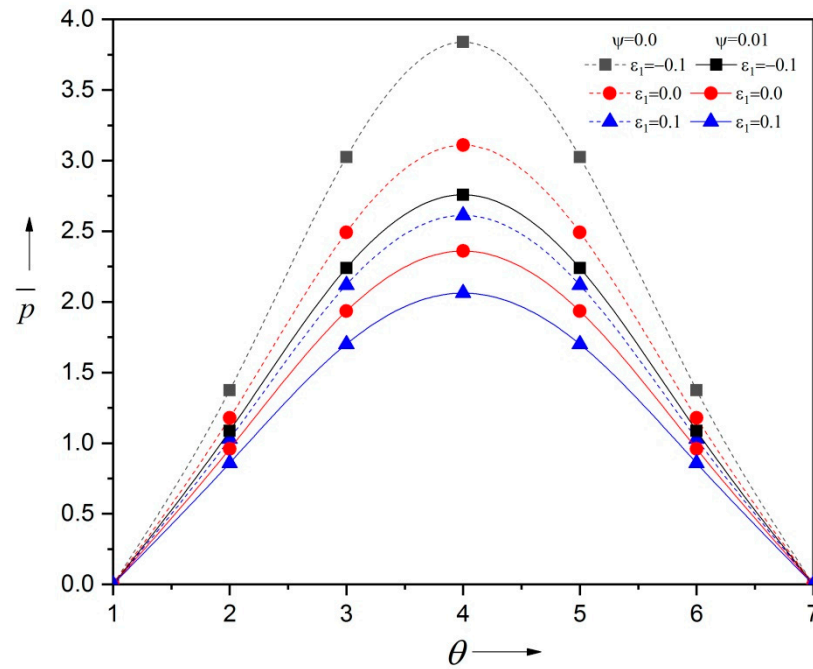


**Figure 6.** Variation in dimensionless pressure  $\bar{p}$  with  $\theta$  for various values of  $\epsilon_1$  and  $\psi$  when  $\sigma = 0.15$ ,  $\alpha = 0.01$ ,  $Q = 0.5$ ,  $\bar{l} = 0.2$ , and  $N = 0.7$ .

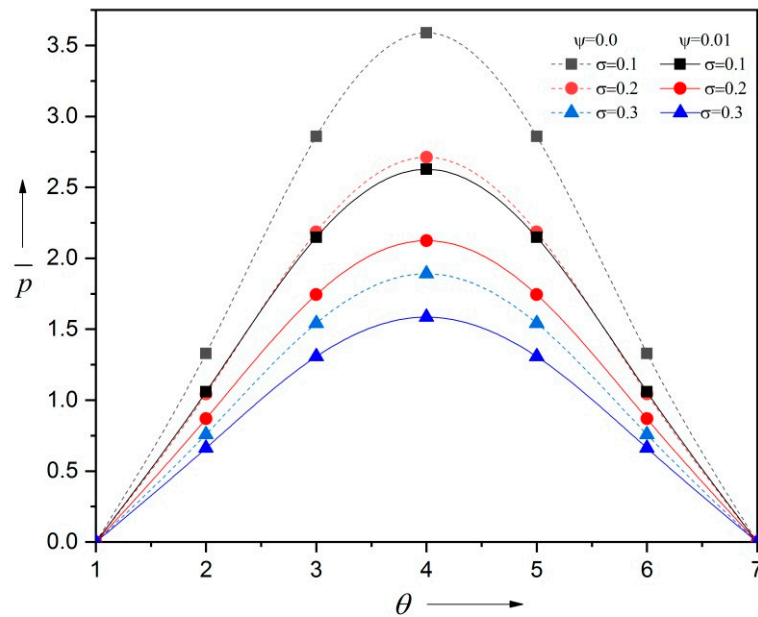


**Figure 7.** Variation in dimensionless pressure  $\bar{p}$  with of  $\theta$  for different values of  $\sigma$  and  $\psi$  when  $\epsilon_1 = -0.01$ ,  $\alpha = 0.01$ ,  $Q = 0.5$ ,  $\bar{l} = 0.2$ . and  $N = 0.7$ .

#### 4.2. Load Capacity

The changes in the dimensionless load capacity  $\bar{W}$  and eccentricity ratio factor  $\epsilon$  are shown in Figure 8 for different values of the viscosity parameter  $Q$ . Here, the eccentricity ratio factor  $\epsilon$  increases the load capacity. Moreover, we confirmed that the variation in viscosity decreases the load capacity more in porous than in solid regions. The variation in  $\bar{W}$  with  $\epsilon$  for distinct values of  $\bar{l}$  and permeability factor  $\psi (= 0.0, 0.01)$  is shown in Figure 9. Notably, increases in  $\bar{l}$  improves  $\bar{W}$  compared to the related Newtonian case ( $l \rightarrow 0$ ). The changes in  $\bar{W}$  with  $\epsilon$  for distinct values of  $N$  and permeability parameter  $\psi (= 0.0, 0.01)$  are noted in Figure 10. Clearly, increasing the value of  $N$  enhances  $\bar{W}$  for both values of  $\psi$ .

While micropolar lubricant improvements result in higher film pressure, improving the integrated load. The load capacity diminishes with rising values of permeability factor  $\psi$ . As a consequence, the porous surface of the bearing provides an alternative channel for lubricant flow, where the higher the permeability, the more likely lubricant is to flow within the porous matrix rather than over the gaps in the film, which thus induces a reduction in  $\bar{W}$ . Figures 11–13 depict the variations in the dimensionless load capacity with eccentricity ratio factor  $\varepsilon$  for various values of roughness parameters  $\alpha$ ,  $\varepsilon_1$ , and  $\sigma$ , respectively. Figures 11 and 12 show that the load capacity diminishes with rising  $\varepsilon$ , decreases for positively rising values of  $\alpha$  and  $\varepsilon_1$  in the porous region compared with the solid region, and improves for decreasing values of  $\alpha$  and  $\varepsilon_1$  in the solid region compared to the porous region. Furthermore, this  $\bar{W}$  decreases with increasing values of  $\sigma$  in the porous region compared to solid region, as evidence in Figure 13.

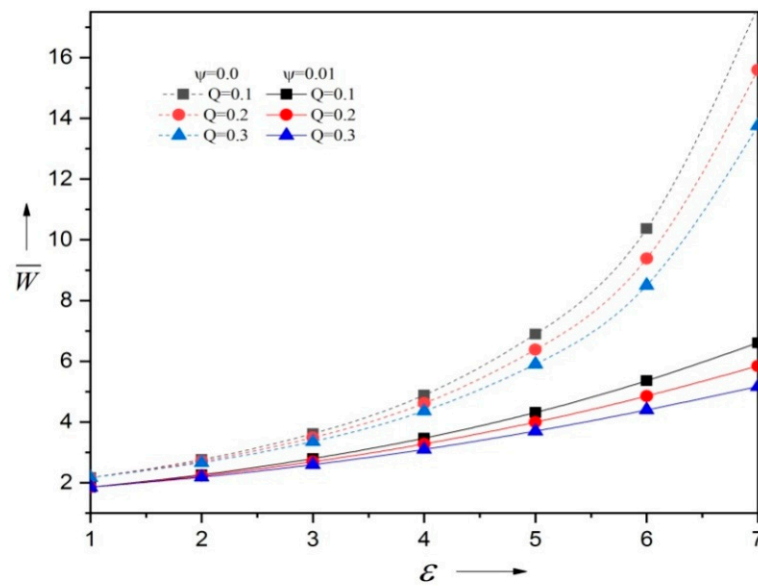


**Figure 8.** Variation in dimensionless load  $\bar{W}$  with  $\varepsilon$  for distinct values of  $Q$  and  $\psi$  when  $\varepsilon_1 = -0.01$ ,  $\sigma = 0.15$ ,  $\alpha = 0.01$ ,  $Q = 0.5$ ,  $N = 0.7$ , and  $\bar{l} = 0.2$ .

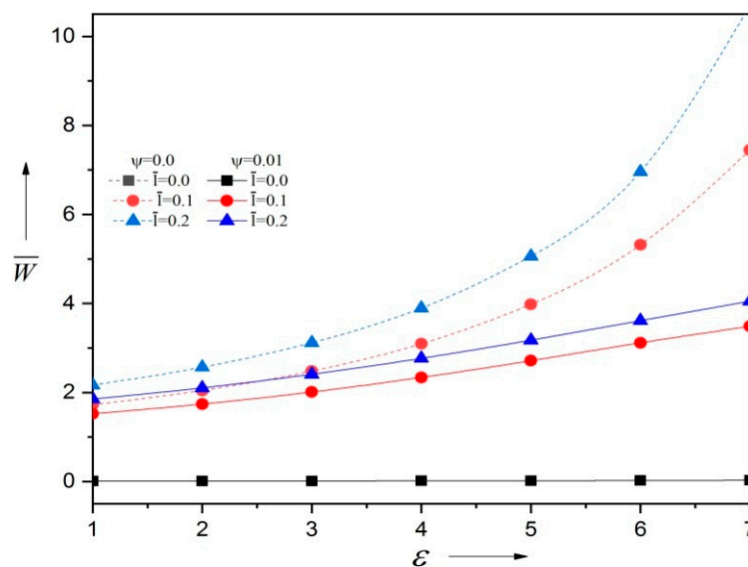


**Figure 9.** Variation in dimensionless load  $\bar{W}$  with  $\varepsilon$  for distinct values of  $\bar{l}$  and  $\psi$  when  $\varepsilon_1 = -0.01$ ,  $\sigma = 0.15$ ,  $\alpha = 0.01$ ,  $Q = 0.5$  and  $N = 0.7$ .

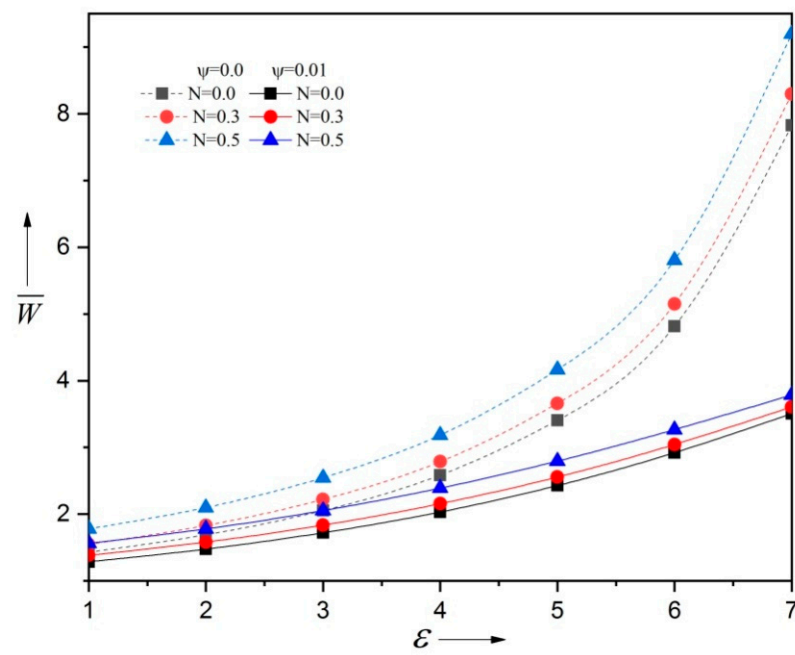


**Figure 10.** Variation in dimensionless load  $\bar{W}$  as a function of  $\epsilon$  for distinct values of  $N$  and  $\psi$  when  $\epsilon_1 = -0.01, \sigma = 0.15, \alpha = 0.01, Q = 0.5$ , and  $\bar{l} = 0.2$ .

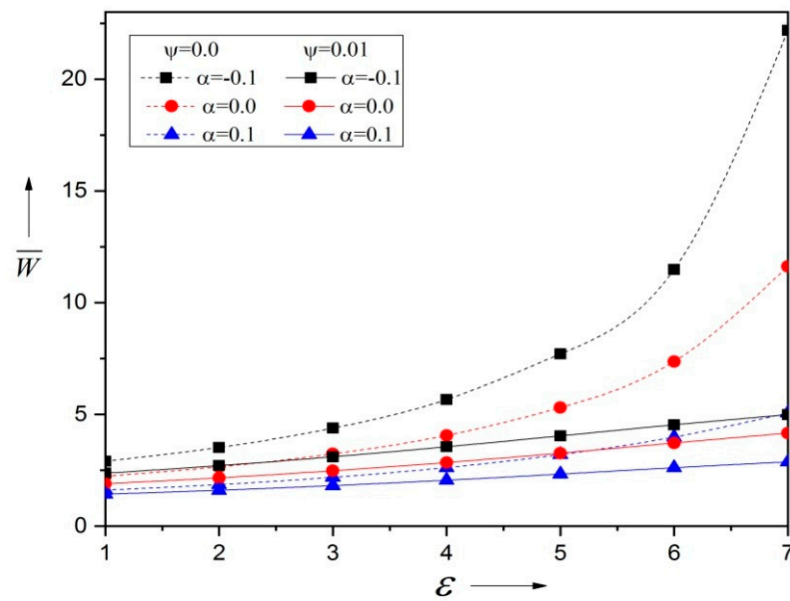


**Figure 11.** Variation in dimensionless load  $\bar{W}$  as a function of  $\epsilon$  for different values of  $\alpha$  and  $\psi$  when  $\epsilon_1 = -0.01, \sigma = 0.15, Q = 0.5, N = 0.7$ , and  $\bar{l} = 0.2$ .

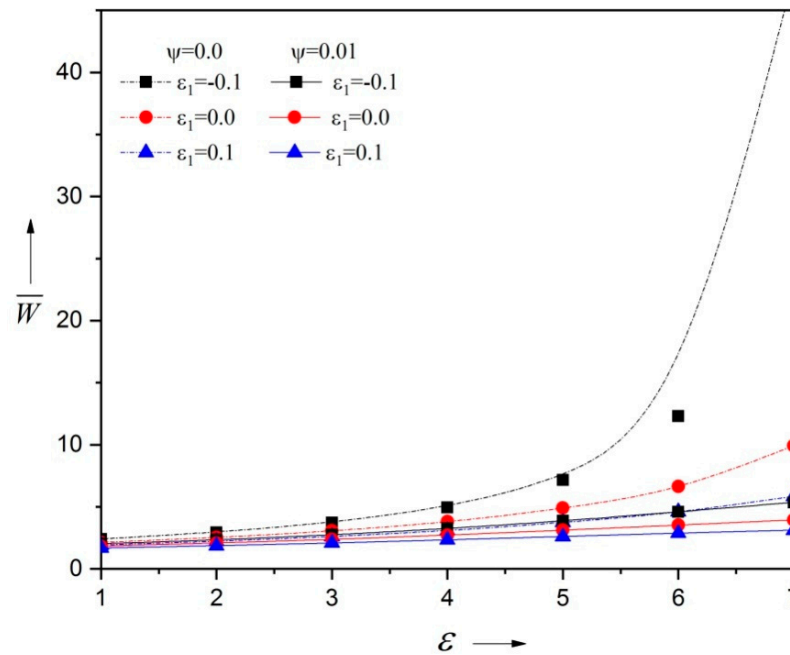


**Figure 12.** Variation in dimensionless load  $\bar{W}$  with  $\epsilon$  for different values of  $\alpha$  and  $\psi$  when  $\alpha = 0.01$ ,  $\sigma = 0.15$ ,  $Q = 0.5$ ,  $N = 0.7$ , and  $\bar{l} = 0.2$ .

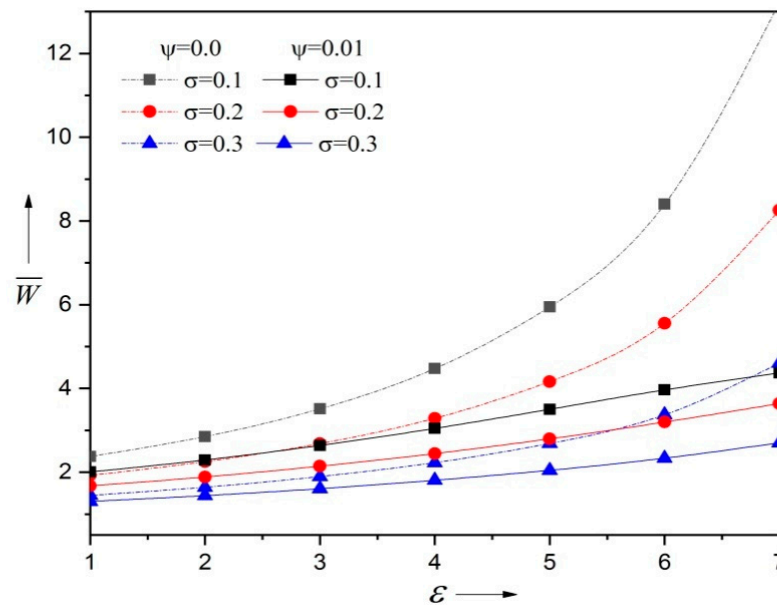


**Figure 13.** Variation in dimensionless load  $\bar{W}$  with  $\epsilon$  for different values of  $\alpha$  and  $\psi$  when  $\alpha = 0.01$ ,  $\sigma = 0.15$ ,  $Q = 0.5$ ,  $N = 0.7$ , and  $\bar{l} = 0.2$ .

#### 4.3. Journal Center Velocity

The impact of  $Q$ , the viscosity variation factor, on the variation in the velocity of the journal center,  $\frac{d\epsilon}{dt}$ , and two values of the permeability factor  $\psi$  when  $\bar{l} = 0.2$ ,  $N = 0.7$ ,  $S' = 1.8$ ,  $\alpha = 0.01$ ,  $\epsilon_1 = -0.01$ , and  $\sigma = 0.15$  with the dimensionless time parameter  $\tau$  with fixed roughness parameters is shown in Figure 14. Interestingly, it should be noted that the variations in viscosity increase the journal center's velocity. The journal center ( $\frac{d\epsilon}{dt}$ ) velocity increases as the permeability parameter  $\psi$  rises. The impact of roughness factors  $\alpha$ ,  $\sigma$ , and  $\epsilon_1$  on the variance in  $\frac{d\epsilon}{dt}$  with respect to the time parameter  $\tau$  for two values of the permeability factor  $\psi$  is presented, respectively, in Figures 15–17. It can be noticed that the increase in the journal center velocity is caused by the positively skewed surface roughness

in the porous region as compared to the solid region, whereas a negatively skewed bearing surface roughness strongly resists increases in the journal center's velocity.

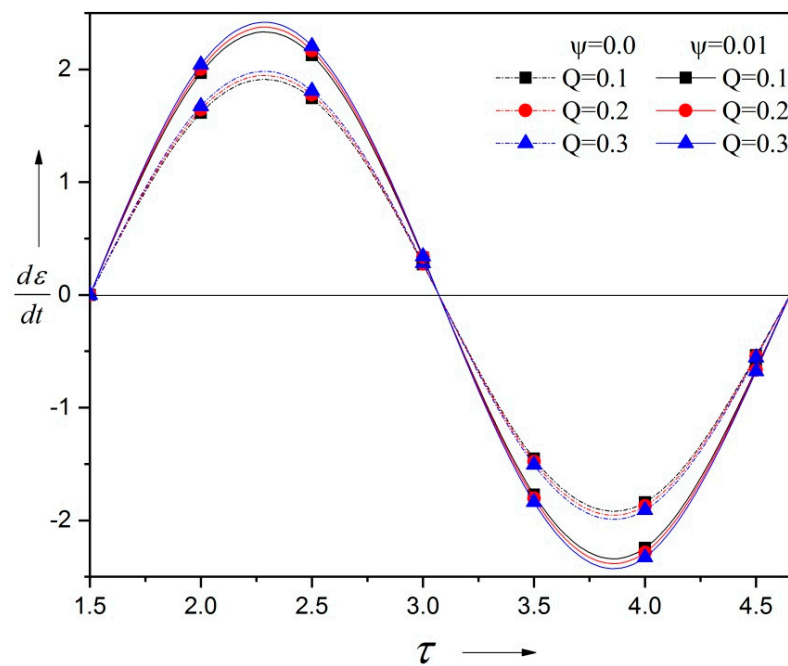


**Figure 14.** Journal center velocity  $\frac{d\varepsilon}{dt}$  versus  $\tau$  for distinct values of the viscosity variation factor  $Q$  and  $\psi$  when  $\sigma = 0.15, \alpha = 0.01, N = 0.7, S' = 1.8, \varepsilon_1 = -0.01,$  and  $\bar{l} = 0.2$ .

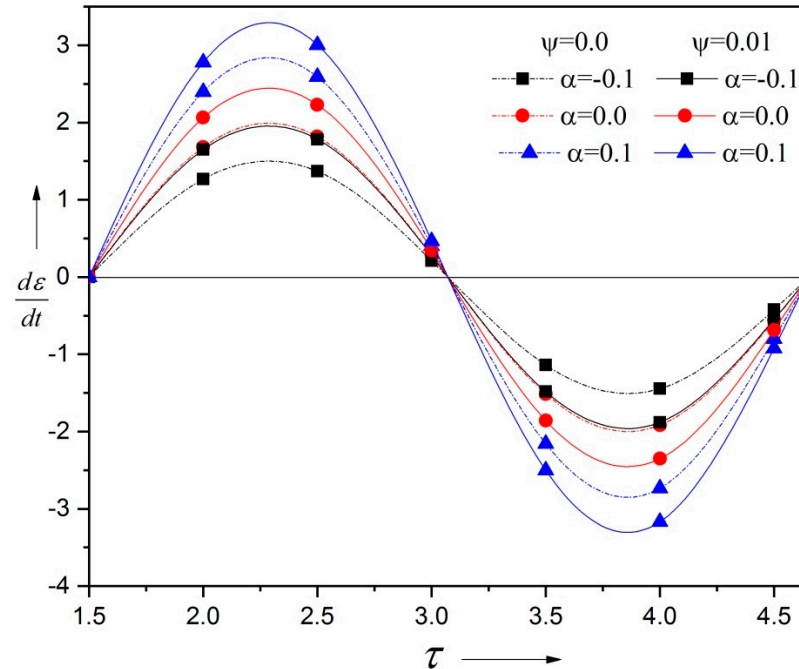


**Figure 15.** Journal center velocity  $\frac{d\varepsilon}{dt}$  versus  $\tau$  for distinct values of  $\alpha$  and  $\psi$  when  $\sigma = 0.15, Q = 0.5, N = 0.7, S' = 1.8, \varepsilon_1 = -0.01,$  and  $\bar{l} = 0.2$ .



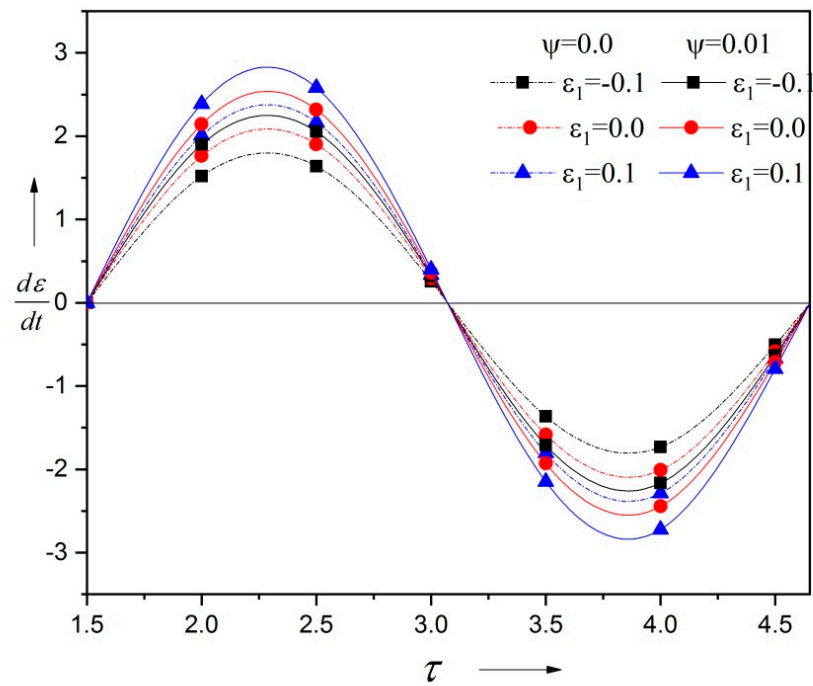


**Figure 16.** Journal center velocity  $\frac{d\varepsilon}{dt}$  versus  $\tau$  for distinct values of  $\varepsilon_1$  and  $\psi$  when  $\sigma = 0.15$ ,  $Q = 0.5$ ,  $N = 0.7$ ,  $S' = 1.8$ ,  $\alpha = 0.01$ , and  $\bar{l} = 0.2$ .

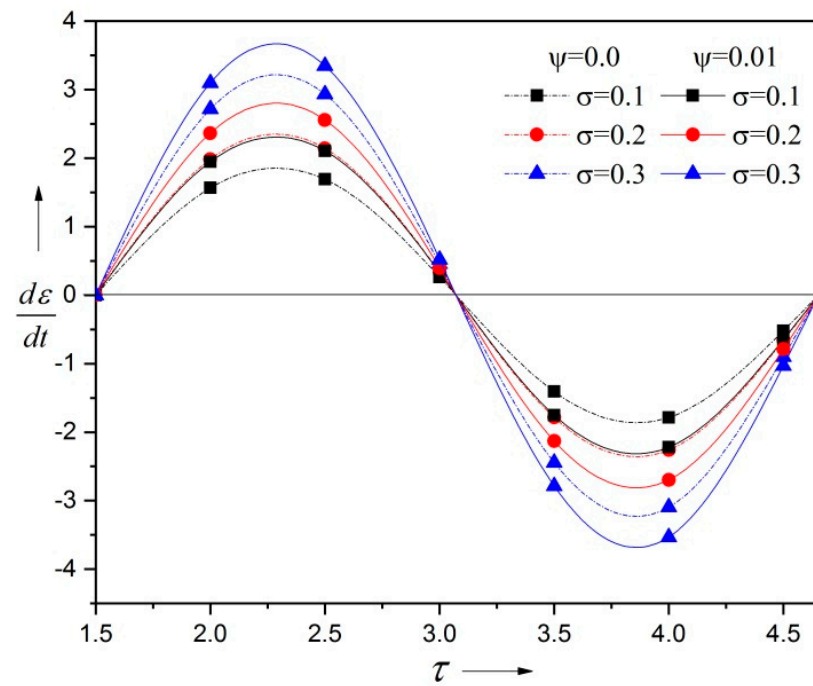


**Figure 17.** Velocity of journal center  $\frac{d\varepsilon}{dt}$  versus  $\tau$  for various values pf  $\sigma$  and  $\psi$  when  $\varepsilon_1 = -0.01$ ,  $Q = 0.5$ ,  $N = 0.7$ ,  $S' = 1.8$ ,  $\alpha = 0.01$ , and  $\bar{l} = 0.2$ .

Table 1 shows the relative percentage increase/decrease in the maximum pressure, load, and journal center velocity for different values of the material parameters and different values of the viscosity variation parameter, as follows:

$$R_{p_{\max}} = \frac{(P_{\max})_{\text{variableViscosity}} - (P_{\max})_{\text{ConstantViscosity}}}{(P_{\max})_{\text{variableViscosity}}} \times 100, R_W = \frac{W_{\text{VariableViscosity}} - W_{\text{ConstantViscosity}}}{W_{\text{VariableViscosity}}} \times 100$$

$$R_{\frac{\partial \epsilon}{\partial t}} = \frac{\left(\frac{\partial \epsilon}{\partial t}\right)_{\text{VariableViscosity}} - \left(\frac{\partial \epsilon}{\partial t}\right)_{\text{ConstantViscosity}}}{\left(\frac{\partial \epsilon}{\partial t}\right)_{\text{VariableViscosity}}} \times 100$$

**Table 1.** Relative percentage increase/decreases in maximum pressure ( $P_{\max}$ ),  $R_{p_{\max}}$ , load carrying capacity  $R_W$ , and journal center velocity  $R_{\frac{\partial \epsilon}{\partial t}}$  for different values of the viscosity variation parameter.

$\psi$	$l = 0.0$				$l = 0.2$		
	$Q$	$R_{p_{\max}}$	$R_W$	$R_{\frac{\partial \epsilon}{\partial t}}$	$R_{p_{\max}}$	$R_W$	$R_{\frac{\partial \epsilon}{\partial t}}$
$\psi = 0.0$	0.1	−4.14	−13.18	1.82	−4.14	−13.40	1.83
	0.2	−8.45	−28.07	3.62	−8.45	−28.59	3.62
	0.3	−12.93	−44.90	5.38	−12.93	−45.79	5.39
$\psi = 0.01$	0.1	−4.14	−13.18	1.82	−4.14	−13.09	1.83
	0.2	−8.45	−28.09	3.62	−8.45	−27.86	3.62
	0.3	−12.93	−44.92	5.38	−12.93	−44.54	5.39

### 5. Conclusions

In this paper, the impact of variations in porosity and viscosity on the dynamic and static characteristics of a rough short journal bearing lubricated with a micropolar fluid under squeezing action was examined on the basis of Eringen’s micropolar fluid theory. The conclusions obtained are based on numerical computation, which are as follows:

- Increases in the viscosity variation parameter decrease the squeeze film pressure and load carrying capacity by 4.14% and 13.14%, respectively, while it enhances the journal center velocity by 1.83%.
- Micropolar lubricants improve the load capacity and film pressure and reduce the journal center velocity under a cyclic load as compared to the related Newtonian case.
- The increase in the porosity factor decreases the squeeze film pressure and load capacity and raises the journal center velocity.
- The presence of a negatively skewed rough surface increases the load capacity and pressure on the squeeze film, whereas the load capacity and squeeze film pressure diminish for positively increasing values of the roughness parameters.
- The velocity of the journal center improves with positively increasing values and decreases for decreasing values of the roughness parameters.
- Our findings align with those obtained by Naduvanamani and Kashinath [40] in the case with no variation in the viscosity parameter, which verifies the effect of variations in the viscosity on rough short porous journal bearings.

**Author Contributions:** Conceptualization, B.K.K. and N.B.N.; methodology, B.K.K.; Wolfram Mathematics software, B.K.K. and N.B.N.; validation, B.K.K. and N.B.N.; formal analysis, B.K.K. and N.B.N.; writing—original draft preparation, B.K.K. and N.B.N.; writing—review and editing, N.B.N.; supervision. All authors have read and agreed to the published version of the manuscript.

**Funding:** This research received no external funding.

**Data Availability Statement:** The original contributions presented in the study are included in the article, further inquiries can be directed to the corresponding author.

**Acknowledgments:** The authors are thankful to the referees for their valuable comments on the earlier draft of this article.

**Conflicts of Interest:** The authors declare no conflicts of interest.

## Nomenclature

$E$	expectancy operator
$E(W(t))$	mean load capacity
$e$	Eccentricity
$c$	radial clearance
$c^*$	maximum deviation from mean film thickness
$h_s^*$	random variable
$h(\theta)$	mean film thickness ( $= c(1 + \varepsilon \cos \theta)$ )
$H$	film thickness ( $= h(\theta) + h_s^*$ )
$H_0$	porous layer thickness
$k$	permeability of porous medium
$l$	characteristic length of polar suspension ( $= \left(\frac{\gamma}{4\mu}\right)^{\frac{1}{2}}$ )
$\bar{l}$	dimensionless form of $\bar{l}$ ( $= \left(\frac{l}{c}\right)$ )
$L$	length of bearing
$N$	coupling number ( $= \left(\frac{\chi}{\chi+2\mu}\right)^{\frac{1}{2}}$ )
$p$	pressure of lubricant
$p_1^*$	porous matrix's pressure
$\bar{p}$	dimensionless mean pressure ( $= \frac{E(p)c^2}{\mu R^2 \left(\frac{dh}{dt}\right)}$ )
$R$	journal radius
$S'$	Sommerfeld number ( $= \frac{\mu N}{\frac{W_0}{2LR}} \left(\frac{R}{c}\right)^2$ )
$t$	Time
$u, v, w$	fluid velocity components in $x, y,$ and $z$ directions
$v_1^*, v_2^*, v_3^*$	microrotational velocity components along $x, y,$ and $z$ directions, respectively
$V$	squeeze velocity $\frac{\partial h}{\partial t}$ ( $= c \left(\frac{d\varepsilon}{dt}\right) \cos \theta$ )
$\bar{W}$	dimensionless mean load capacity ( $= \frac{E(W(t))}{\mu LR \left(\frac{dh}{dt}\right)}$ )
$W_0$	applied cyclic load's amplitude
$W_s$	mean steady load
$x, y, z$	rectangular coordinates
$\alpha$	dimensionless form regarding $\alpha_1^*$ ( $= \frac{\alpha_1^*}{c}$ )
$\alpha_1^*$	stochastic mean film thickness
$\gamma, \chi$	viscosity coefficients for micropolar fluids
$\varepsilon$	eccentricity ratio factor ( $= \frac{e}{c}$ )
$\varepsilon_1$	dimensionless form of $\varepsilon_1^*$ ( $= \frac{\varepsilon_1^*}{c^3}$ )
$\varepsilon_1^*$	measure of symmetry about random stochastic variable
$\mu$	lubricant viscosity
$\psi$	permeability parameter ( $= \frac{k_1^* H_0}{c^3}$ )
$\sigma^2$	dimensionless form of $\sigma_1^{*2}$ ( $= \frac{\sigma_1^{*2}}{c^2}$ )
$\sigma_1^{*2}$	Variance

## References

1. Lord Rayleigh, O.M.F.R.S. I. Notes on the theory of lubrication. *Lond. Edinb. Dublin Philos. Mag. J. Sci.* **1918**, *35*, 1–12. [CrossRef]
2. Cameron, A.; Wood, W.L. The full journal bearings. *Proc. Inst. Mech. Eng.* **1949**, *161*, 59. [CrossRef]
3. Tipei, N. *Theory of Lubrication*; Stanford University Press: Stanford, CA, USA, 1962; Chapter 3.
4. Lidia, G.; Jaroslaw, S.; Artur, O.; Tomasz, Z. Experimental investigation into surface texture effect on journal bearings performance. *Tribol. Int.* **2019**, *136*, 372–384. [CrossRef]
5. Allaire, P.E.; Flack, R.D. *Design of Journal Bearings for Rotating Machinery*; Texas A&M University. Turbomachinery Laboratories: College Station, TX, USA, 1981; pp. 25–45. Available online: <https://hdl.handle.net/1969.1/163716> (accessed on 10 November 2024).
6. Sunil, K.; Vijaya, K.; Anoop, K. Influence of lubricants on the performance of journal bearings. *Tribol.-Mater. Surf. Interfaces* **2020**, *14*, 67–78. [CrossRef]

7. Eringen, A.C. Simple micropolar fluids. *Int. J. Eng. Sci.* **1964**, *2*, 205–217. [CrossRef]
8. Eringen, A.C. Theory of micropolar fluids. *J. Math. Mech.* **1966**, *16*, 1–18. Available online: <https://www.jstor.org/stable/24901466> (accessed on 10 November 2024). [CrossRef]
9. Allen, S.J.; Kline, K.A. Lubrication theory for micropolar fluids. *J. Appl. Mech.* **1971**, *38*, 646–650. [CrossRef]
10. Zaheeruddin, K.H.; Isa, M. Micropolar fluid lubrication of one-dimensional journal bearing. *Wear* **1978**, *50*, 211–220. [CrossRef]
11. Tipei, N. Lubrication with micropolar liquids and its application to short journal bearings. *J. Tribol.* **1979**, *101*, 356–363. [CrossRef]
12. Bujurke, N.M.; Bhavi, S.G.; Hiremath, P.S. Squeeze film lubricated with micropolar fluids. *Proc. Indian Natl. Sci. Acad.* **1987**, *53*, 391–398.
13. Sharma, S.; Lambha, S.; Mittal, V.; Verma, R. Micropolar lubricant effects on the performance of partial journal bearings. *Proc. Inst. Mech. Eng. Part J J. Eng. Tribol.* **2023**, *237*, 1461–1470. [CrossRef]
14. Boualem, C.; Mohamed, H.; Othman, T.; Moussa, S. Combined effects of elastic deformation and piezo-viscous dependency on the performance of a journal bearing operating with a non-Newtonian fluid. *Proc. Inst. Mech. Eng. Part J J. Eng. Tribol.* **2022**, *236*, 2457–2467. [CrossRef]
15. Murti, P.R.K. Lubrication of finite porous journal bearing. *Wear* **1973**, *26*, 95–104. [CrossRef]
16. Li, W.L. Derivation of modified Reynolds equation—a porous media model. *J. Tribol.* **1999**, *121*, 823–829. [CrossRef]
17. Anas, S.; Mohamed, N.; Mohamed, E.K. Non-Newtonian effects on porous elastic journal bearings. *Tribol. Int.* **2018**, *120*, 23–33. [CrossRef]
18. Dhanapal, P.; Kanguri, S.; Hanumagowda, B. Squeeze film lubrication on porous secant curved circular plates induced by micropolar fluids. *AIP Conf. Proc.* **2023**, *1*, 2852. [CrossRef]
19. Bhattacharjee, B.; Chakraborti, P.; Choudhuri, K. Theoretical analysis of single layered porous short journal bearing under the lubrication of micropolar fluid. *J. Braz. Soc. Mech. Sci. Eng.* **2019**, *41*, 365. [CrossRef]
20. Bhattacharjee, B.; Biswas, N.; Chakraborti, P. A comparative analysis of the performance of micropolar fluid lubricated single layered and double-layered porous journal bearing. *J. Porous Media* **2022**, *25*, 35–45. [CrossRef]
21. Christensen, H. Stochastic models of hydrodynamic lubrication of rough surfaces. *Proc. Inst. Mech. Eng.* **1969**, *184*, 1013–1026. [CrossRef]
22. Zhu, S.; Zhang, X.; Sun, J.; Wang, D. A study of misaligned compliant journal bearings lubricated by non-Newtonian fluids considering surface roughness. *Tribol. Int.* **2023**, *179*, 108138. [CrossRef]
23. Naduvinamani, N.B.; Ashwini, A. Surface roughness influence on the dynamic performance Rayleigh step bearing lubricated with couple stress fluid. *Proc. Natl. Acad. Sci. India Sect. A Phys. Sci.* **2024**, *94*, 235–247. [CrossRef]
24. Monayya, M.; Santosh, S. Micropolar fluid lubrication of finite partial rough porous journal bearings with squeeze effect. *Int. J. Mech. Eng. Technol.* **2015**, *6*, 258–279.
25. Chaithra, N.; Hanumagowda, B.; Sreekala, C.; Vasanth, K. Study about the characteristics of squeeze film between rough porous curved annular plates in the presence of micropolar fluids. *Mater. Today Proc.* **2023**, *in press*. [CrossRef]
26. Ujjal, B.; Sanjoy, D.; Santanu, D. Influence of Roughness on Micropolar Lubricated Finite Porous Journal Bearing. In *Recent Advances in Thermofluids and Manufacturing Engineering*; Springer Nature: Singapore, 2022; pp. 543–559. [CrossRef]
27. Sinha, P.; Singh, C.; Prasad, K.R. Effect of viscosity variation due to lubricant additives in journal bearings. *Wear* **1981**, *66*, 175–188. [CrossRef]
28. Rao, P.S.; Kumar Rahul, A. Effect of viscosity variation on non-Newtonian lubrication of squeeze film conical bearing having porous wall operating with Rabinowitsch fluid model. *Proc. Inst. Mech. Eng. Part C J. Mech. Eng. Sci.* **2018**, *237*, 2538–2551. [CrossRef]
29. Zheng, L.; Zhu, H.; Zhu, J.; Deng, Y. Effect of oil film thickness and viscosity on the performance of misaligned journal bearings with couple stress lubricants. *Tribol. Int.* **2020**, *146*, 106229. [CrossRef]
30. Rahul, A.K.; Singh, M.K.; Saha, S. Squeeze film lubrication analysis and optimization of porous annular disk with viscosity variation of non-Newtonian fluid: Rabinowitsch fluid model. *Tribol. Int.* **2023**, *179*, 108060. [CrossRef]
31. Awati, V.B.; Kengangutti, A.; Kumar, M. Multigrid method for the solution of combined effect of viscosity variation and surface roughness on the squeeze film lubrication of Journal bearings. *J. Mech. Eng.* **2016**, *46*, 1–8. [CrossRef]
32. Lin, J.R. Static and dynamic behaviours of pure squeeze films in couple stress fluid lubricated short journal bearings. *Proc. Inst. Mech. Eng. Part J J. Eng. Tribol.* **1997**, *211*, 29–36. [CrossRef]
33. Gu, Y.; Cheng, J.; Xie, C.; Li, L.; Zheng, C. Theoretical and numerical investigation on static characteristics of aerostatic porous journal bearings. *Machines* **2022**, *10*, 171. [CrossRef]
34. Dang, R.K.; Goyal, D.; Chauhan, A.; Dhama, S.S. Effect of non-Newtonian lubricants on static and dynamic characteristics of journal bearings. *Mater. Today Proc.* **2020**, *28*, 1345–1349. [CrossRef]
35. Fang, C.; Zhu, A.; Zhou, W.; Peng, Y.; Meng, X. On the stiffness and damping characteristics of line contact under transient elastohydrodynamic lubrication. *Lubricants* **2022**, *10*, 73. [CrossRef]
36. Fu, C.; Zhu, W.; Ma, J.; Gu, F. Static and dynamic characteristics of journal bearings under uncertainty: A Nonprobabilistic perspective. *J. Eng. Gas. Turbines Power* **2022**, *144*, 071012. [CrossRef]
37. Jaya Chandra Reddy, G.; Eswara Reddy, C.; Rama Krishna Prasad, K. Effect of viscosity variation on the squeeze film performance of a narrow hydrodynamic journal bearing with couple stress fluid. *Proc. Inst. Mech. Eng. Part J J. Eng. Tribol.* **2008**, *2*, 222. [CrossRef]

38. Ajimokotan, H.A. Viscosity of Fluid Lubricants. In *Principles and Application of Tribology*; Springer Nature: Cham, Switzerland, 2024; pp. 29–37.
39. Sharma, S.; Krishna, C.M. Static and dynamic performances of an offset bearing under a micropolar lubricant. *Proc. Inst. Mech. Eng. Part J J. Eng Tribol* **2022**, *236*, 59–69. [[CrossRef](#)]
40. Naduvinamani, N.B.; Kashinath, B. Surface-roughness effects on the static and dynamic behaviour of squeeze film lubrication of short journal bearing with micpolar fluids. *Proc. Inst. Mech. Eng. Part J J. Eng. Tribology*. **2008**, *222*, 121–131. [[CrossRef](#)]
41. Andharia, P.I.; Gupta, J.L.; Deheri, G.M. Effect of surface roughness on hydrodynamic lubrication of slider bearings. *Trans. Tribol.* **2001**, *44*, 291–297. [[CrossRef](#)]
42. Naduvinamani, N.B.; Santosh, S. Micropolar fluid squeeze film lubrication of finite porous journal bearing. *Tribol. Int.* **2011**, *44*, 409–416. [[CrossRef](#)]

**Disclaimer/Publisher’s Note:** The statements, opinions and data contained in all publications are solely those of the individual author(s) and contributor(s) and not of MDPI and/or the editor(s). MDPI and/or the editor(s) disclaim responsibility for any injury to people or property resulting from any ideas, methods, instructions or products referred to in the content.